

impurity concentration C which is determined by the probabilities of the elementary processes of growth and doping of a crystal,

$$C^* = \alpha(\rho_1 C_2) \alpha(C_1 N_s) / \alpha(\rho_1 N_s) \alpha(C_1 C_2). \quad (24)$$

The effect of limitation of the concentration C arises under the condition that $N_s \ll C_2$, when almost all the impurity arriving at the surface is desorbed in the form of dimers. Then δ can be much less than unity. The effect of limitation of the concentration P was experimentally found in Ref. 1. Experimental investigations of the dependence of C^* on temperature and on the growth rate would enable us to obtain additional information on the

elementary processes of growth and doping of diamond-like crystals.

¹V. P. Kuznetsov and V. V. Postnikov, *Kristallografiya* **19**, 346 (1974) [Sov. Phys. Crystallogr. **19**, 211 (1974)].

²M. I. Ovsyannikov, A. S. Perov, and V. V. Postnikov, in: *Electronic Properties of Solids and Phase Transitions* [in Russian], Mordovsk. Univ., Saransk (1978), p. 36.

³A. S. Perov and V. V. Postnikov, *Kristallografiya* **27**, 1162 (1982) [Sov. Phys. Crystallogr. **27**, 697 (1982)].

⁴A. S. Perov, *Izv. Vyssh. Uchebn. Zaved., Fiz.*, No. 12, 92 (1981).

⁵A. A. Chernov, E. I. Givargizov, Kh. S. Bagdasarov, et al., *Contemporary Crystallography* [in Russian], Vol. 3, Nauka, Moscow (1980).

Translated by S. G. Kirsch

Motion of a plane front during crystallization

A. R. Umantsev

Institute of Metallurgy and Physics of Metals, and Central Scientific-Research Institute of Ferrous Metallurgy

(Submitted August 29, 1983)

Kristallografiya **30**, 153-160 (January-February 1985)

The authors suggest ^(asymptotic) a procedure for obtaining solutions to an integral equation representing the motion of a plane phase boundary in growth of a crystal by the normal mechanism. The problem is solved by means of a numerical model. ^(also)

INTRODUCTION

Many authors have studied the growth rates of crystals with a plane front. It is known that, if the advance of the boundary is determined by deviation of its state from equilibrium, then various regimes can be realized in the system, depending on the external conditions.^{1,2} However, they have not yet been obtained as different solutions of a single problem. In our work, the integral equation representing normal growth of a crystal is solved by means of an asymptotic expansion by the method of Laplace. In the second part we construct an algorithm for obtaining numerical solutions to the problem of solidification, and compare these with the analytical results.

ASYMPTOTIC METHOD

It is known that advance of a plane front of crystallization along the x axis, perpendicular to its plane, can be represented by the inhomogeneous equation of heat conduction,³

$$C \frac{\partial T}{\partial t} = \lambda \frac{\partial^2 T}{\partial x^2} + Lv \delta[x - y(t)], \quad (1)$$

where C and L are respectively the specific heat and latent heat of transition of unit volume, λ is the thermal conductivity of the medium, which is the same in both phases (as also is C), and $T(x, t)$ is the temperature of the medium at time t and at the point with coordinate x . At time t , the phase boundary, advancing at a velocity $v(t)$, has the coordinate $x = y(t)$, where

$$y(t) = \int_{t_0}^t v(\tau) d\tau. \quad (2)$$

The delta function shows that heat is emitted only in a narrow region near this point. In the classical problem of Stefan it is required that the temperature at the surface of the front $T_I = T[y(t), t]$ is equal to the phase equilibrium temperature T_M , and the normal mechanism of growth relates these quantities with the boundary advance rate⁴ as follows:

$$v = \mu(T_M - T_I) \quad (3)$$

where μ is the kinetic growth coefficient.

It is known that the solution of Eq. (1) satisfies Stefan's condition at the phase boundary,

$$\lambda \left. \frac{\partial T}{\partial x} \right|_{x=y(t)-0} - \lambda \left. \frac{\partial T}{\partial x} \right|_{x=y(t)+0} = Lv(t). \quad (4)$$

For an unbounded region $-\infty < x < \infty$ with the initial condition $T(x, t_0) = T_L < T_M$, corresponding to supercooling of the system, the solution of Eq. (1) can be written with the aid of the fundamental solution of the equation of heat condition,^{5,6}

$$\begin{aligned} T(x, t) &= T_L + \int_{t_0}^t \int_{-\infty}^{\infty} \frac{L}{C} v(\tau) \delta[\xi - y(\tau)] \exp \left[-\frac{(x - \xi)^2}{4\alpha(t - \tau)} \right] \frac{d\xi d\tau}{2\sqrt{\pi\alpha(t - \tau)}} \\ &= T_L + \frac{L}{C} \int_{t_0}^t \exp \left\{ -\frac{[x - y(\tau)]^2}{4\alpha(t - \tau)} \right\} \frac{v(\tau) d\tau}{2\sqrt{\pi\alpha(t - \tau)}}, \end{aligned} \quad (5)$$

where $\alpha = \lambda/C$ is the thermal diffusivity of the medium.

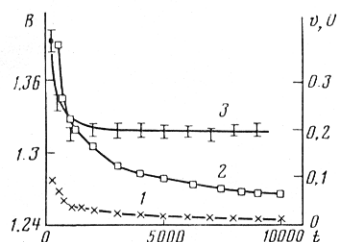


FIG. 5. Time dependences of v (1), U (2), and B (3) at $\Delta\theta = 0.8$.

When $\Delta\theta < 1$ and $t \rightarrow \infty$, the right-hand side of (12) tends to $+\infty$ and the expression for the velocity asymptotically tends to

$$v = \beta \sqrt{\alpha/t}. \quad (14)$$

Here $\beta = [2(1 - \Delta\theta)]^{-1/2}$ and β coincides with the solution of the transcendental equation of the Cauchy-Stefan problem,⁹

$$(\sqrt{\pi}/2)\beta \exp \beta^2 (1 - \operatorname{erf}^2 \beta) = \Delta\theta \quad (15)$$

for large β . For small values of β , owing to condition (10) our expansion is not exact, and the exact value of β can be obtained by direct substitution of solution (14) into Eq. (8). The result is the same as (15).

When $\Delta\theta = 1$, the solution to Eq. (11) takes the form

$$v = \left(\frac{\alpha v_0}{3t} \right)^{1/3} \quad \bar{v} = \left(\frac{2v_0}{3t} \right)^{1/3} \quad (16)$$

It is intermediate between the solutions (7) and (14). A similar result was proposed in Ref. 10 on the basis of an analysis of the approximate solution of the diffusion problem of isothermal crystallization of a binary alloy.

Taking three terms in the expansion of the integral in (8) with respect to $v^2 t / 4\alpha$, we obtain the equation

$$1 + \frac{v}{v_0} + \alpha \frac{v'}{v^3} + \alpha^2 \left[15 \left(\frac{v'}{v^3} \right)^2 - 4 \frac{v''}{v^5} \right] = \Delta\theta. \quad (17)$$

This has the same stationary solution (7) with the same limitation $\Delta\theta > 1$. When $\Delta\theta < 1$ it has an asymptotic solution (14) in which β is subject to the equation

$$1 - \frac{1}{2\beta^2} + \frac{3}{4\beta^4} = \Delta\theta,$$

which is the next approximation in the expansion of (15) in $1/\beta$.

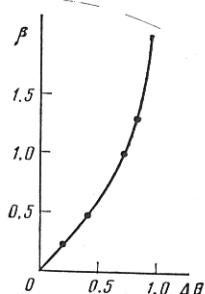


FIG. 6. Dependence of β on supercooling $\Delta\theta$. Solid curve: β vs $\Delta\theta$ for Cauchy-Stefan problem.

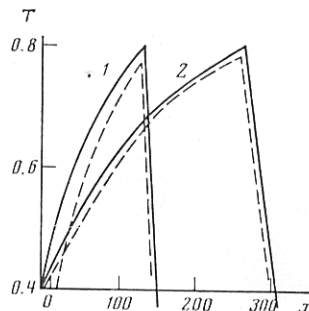


FIG. 7. Temperature distribution in system at $\Delta\theta = 0.8$ for times $t = 2500$ (1) and $10,000$ (2). Solid curves: temperature distribution for Cauchy-Stefan problem; dashed curves: results of numerical model.

When $\Delta\theta = 1$, Eq. (17) has the asymptotic solution

$$t \sim \alpha \left(\frac{v_0}{3v^3} + \frac{1}{2v^2} \right). \quad (18)$$

Thus (16) is an asymptotically exact solution to Eq. (8). This can also be verified by direct substitution of (16) into (8) with $t \rightarrow \infty$. In general, we can prove that for the solution $v \sim t^\gamma$ the n -th term in the expansion is of order

$$I_n \sim \frac{v^{(n)}}{v^{2n+1}} \sim \frac{1}{t^{n(2\gamma+1)}},$$

i.e., when $\gamma > -1/2$ and $t \rightarrow \infty$, the terms with $n > 1$ are not important.

Since in a real system we cannot fix supercooling exactly equal to unity, the question arises of the observability of solution (16). Small undamped fluctuations of the supercooling do not influence the character of the solution at $\Delta\theta > 1$ or $\Delta\theta < 1$, since they alter only the values of the coefficients depending on the supercooling; but they can have a catastrophic influence on solution (16), converting it either to (7) or to (14). To investigate the stability of this solution it is necessary to solve Eq. (8) for a time-dependent supercooling. Instead, we can solve Eq. (11), and the result will be correct if it satisfies condition (10). Changing to the variables $u = (v_0/v)^3$, $\tau = 3t/\tau_0$, $\tau_0 = \alpha/v_0^2$, $\delta(\tau) = \Delta\theta - 1$, from (11) we get the equation

$$\frac{du}{d\tau} = 1 - \delta(\tau) u^{1/3},$$

which, when $\delta(\tau) = 0$, has the solution $u = \tau$. When $\delta(\tau) \neq 0$, writing the solution in the form $u = \tau[1 - r(\tau)]$ and linearizing with respect to $r(\tau)$, we get the equation

$$\tau \frac{dr}{d\tau} + r = \tau^{1/3} \delta(\tau),$$

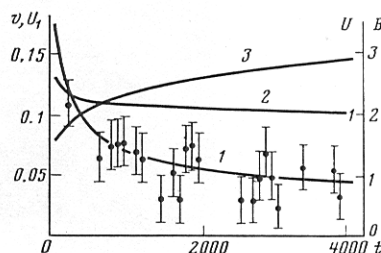


FIG. 8. Variation of v (1), U (2), B (3), and U_1 (points) with time, $\Delta\theta = 1$.

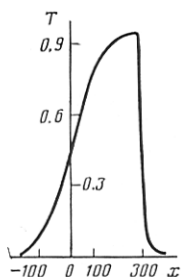


FIG. 9. Temperature distribution in system for $\Delta\theta = 1$ and $t = 4000$.

which has a solution of the form

$$r(\tau) = \frac{1}{\tau} \int_0^\tau \delta(\tau) \tau^{1/2} d\tau.$$

If $\delta(\tau)$ is a small harmonic perturbation, e.g., $\delta(\tau) = \delta_0 \cos \omega\tau$, then $r(\tau) \rightarrow 0$ when $\tau \rightarrow \infty$, i.e., the previous solution (16) is stable relative to these perturbations. But if $\delta(\tau)$ has a constant component, e.g., $\delta(\tau) = \delta_1 + \delta_0 \cos \omega\tau$, then $r(\tau) \rightarrow (3/4)\delta_1 \tau^{1/3}$ when $\tau \rightarrow \infty$, and (16) is not a solution of (11).

Now let us consider the behavior of the system at *early* various times. When $t \rightarrow +0$ the argument of the exponential in (8) tends to zero, and for the velocity we get a linear integral Volterra equation of the second kind,

$$v(t) + v_0 \int_0^t \frac{v(\tau) d\tau}{2\sqrt{\pi\alpha(t-\tau)}} = v_0 \Delta\theta,$$

which has an exact solution of the form

$$v = v_0 \Delta\theta \exp \frac{t}{4\tau_0} \operatorname{erfc} \sqrt{\frac{t}{4\tau_0}}.$$

NUMERICAL MODEL

In the region $-\infty < x < \infty$, $0 < t$, we set up a difference network $\omega_{x,t} = \{x_j, t_K\}$ with intervals $(\Delta x, \Delta t)$ in space and time respectively. The state of a cell lying in the interval $[j\Delta x, (j+1)\Delta x]$ and having unit cross section in a plane perpendicular to the x axis, at time $t_K = K\Delta t$ will be characterized by its mean temperature T_j^K and the ~~portion~~ g_j^K of solid phase, equal to the ratio of crystallized material in the cell to its volume. In all cells behind the front, $g_j^K = 1$, and ahead of the front $g_j^K = 0$, and $0 < g_j^K < 1$ in a surface cell, i.e., one in which the front lies at a given moment. The change in g_j^K in the process of solidification is

$$\Delta g_j^K = \begin{cases} v(t_K) \frac{\Delta t}{\Delta x} & \text{in a surface cell,} \\ 0 & \text{in all other cells,} \end{cases} \quad (19)$$

and $v(t_K)$, the velocity of the boundary at time t_K , satisfies the condition of normal crystal growth (3).

After a time Δt , the quantity of heat emitted in a surface cell is $L\Delta g_j^K \Delta x$, and the change in the temperature of the medium will satisfy the equation of heat balance,

$$C(T_j^{K+1} - T_j^K) = \lambda \frac{\Delta t}{(\Delta x)^2} (T_{j-1}^K + T_{j+1}^K - 2T_j^K) + L\Delta g_j^K. \quad (20)$$

Now let us change to dimensionless variables $\tilde{T}_j^K =$

$C(T_j^K - T_L)/L$, $\tilde{x} = x/\rho_0$, $\tilde{t} = t/\tau_0$, and $\tilde{v} = v/v_0$. For Eq. (20), ρ_0 and τ_0 must satisfy the relationship $\alpha\tau_0/\rho_0^2 = 1$. However, boundary condition (3) imposes an additional condition: $v_0\tau_0/\rho_0 = 1$. Thus

$$\tau_0 = \frac{\alpha C^2}{\mu^2 L^2}, \quad \rho_0 = \frac{\alpha C}{\mu L}, \quad h = \frac{\Delta x}{\rho_0}, \quad \tau = \frac{\Delta t}{\tau_0}, \quad (21)$$

and Eqs. (3), (19), and (20) will give the following system (here and below we omit the tilde signs):

$$T_j^{K+1} = T_j^K + \frac{\tau}{h^2} (T_{j-1}^K + T_{j+1}^K - 2T_j^K) + \Delta g_j^K, \quad (22.1)$$

$$g_j^{K+1} = g_j^K + \Delta g_j^K, \quad (22.2)$$

$$\Delta g_j^K = \xi_j^K \frac{\tau}{h} (\Delta\theta - T_j^K), \quad (22.3)$$

$$\xi_j^K = \begin{cases} 1 & \text{for surface cell,} \\ 0 & \text{for all others.} \end{cases} \quad (22.4)$$

The rate of advance of the front, v , was determined as the ratio of the length h of a cell to the time in which it is traversed. To verify relations (7), (14), and (16) in the scheme we also calculated the functions $B = v\sqrt{t}$ and $U = 3v^3 t$.

The calculations were made for a fixed number of points $N = 1000$. To model the process in an infinite region, the spatial interval h was chosen so that the dimension of the whole region Nh was greater than the thermal length $l = 1/v$ of the temperature field. At the same time, h itself must be less than l . At the boundaries of the region at $N = 0$ and $N = 1000$ we chose boundary conditions of the first kind. The time interval τ must satisfy the condition of stability of the explicit one-dimensional difference scheme $\tau/h^2 \leq 0.5$. Moreover, to increase the accuracy of the calculation we must satisfy the condition $\Delta\theta\tau/h < 1$, so that each cell solidifies over a large number of intervals.

When $t = 0$, in conformity with the initial conditions of the Cauchy-Stefan problem, the temperature of all the cells was put equal to T_L , and the solid phase was taken as the cells with number $1 \leq j \leq 300$.

To solve system (22.1)-(22.4) we compiled a program in FORTRAN-IV. Each realization requires about 30 min on the ES-1022 computer.

Figure 1 plots the results of computation of the velocity for various values of τ and h with $\Delta\theta = 1.2$. The growth rate is practically independent of τ and h over the chosen interval of variation.

For a supercooling $\Delta\theta > 1$, the rate of advance of the boundary, after a time, reaches its quasistationary value (Fig. 2). The time taken to reach a value 5% greater than the asymptotic level (horizontal straight line in Fig. 2) can be reckoned equal to three times the nonstationary time. Figure 3 compares the theoretical [Eqs. (7) and (13)] and numerical dependences of v and τ_n on the supercooling. Figure 4 gives the temperature distributions in comparison with the theoretical values found from Eq. (6).

When $\Delta\theta < 1$, the velocity v and the function U monotonically decrease with time, while the function B tends to a constant value β (Fig. 5), showing that Eq. (14) is correct. The dependence of β on $\Delta\theta$ (Fig. 6) coincides with the theoretical relation (15). The unbounded increase in the kinetic coefficient μ corresponds to the fact that the characteristic time scale τ_0 tends to zero (21) and the dimensionless time t tends to infinity for a fixed true moment of time. Figure 7 shows the temperature profiles for two moments of dimensionless time t in comparison with the temperature distributions of the corresponding Cauchy-Stefan problem. The convergence of these two distributions as $t \rightarrow \infty$ shows that our algorithm converges to Stefan's algorithm as $\mu \rightarrow \infty$.

When $\Delta\theta = 1$ the velocity monotonically decreases with time, while B increases, and U tends to a constant value equal to unity (Fig. 8). This shows that when $\Delta\theta = 1$ and $t \rightarrow \infty$ relation (16) is satisfied. Moreover, if we take account of the next term in the asymptotic expansion for the velocity, then for the function $U_1 = 2(U - 1)/3$ from (18) we get the relation

$$U_1 = v + O(v^2),$$

which is also satisfied in the model (points in Fig. 8). In Fig. 9 we show the temperature distribution in the system when $\Delta\theta = 1$. Numerical modeling automatically proves the stability of the solution, since otherwise errors of computation due to the finite-difference scheme would alter the character of the asymptotic dependence of

the velocity on the time. Thus the results of the model act as a check on both the first and second terms in the asymptotic expansions of the velocity.

We thank V. V. Vinogradov and A. V. Nazarov for discussing the work and giving helpful advice, and D. E. Temkin, who showed that, by analogy with the diffusion problem,¹⁰ the relation $v \sim t^{-1/3}$ must hold when $\Delta\theta = 1$.

¹J. Rosenthal, Trans. ASME **68**, 849 (1946).

²B. Ya. Lyubov, in: Crystal Growth [in Russian], Vol. 5, Nauka, Moscow (1965), p. 100.

³B. V. Petukhov and Y. Estrin, J. Phys. F **10**, 223 (1980).

⁴V. T. Borisov, Dokl. Akad. Nauk SSSR **151**, 1311 (1963) [Sov. Phys. Dokl. **8**, 834 (1964)].

⁵A. N. Tikhonov and A. A. Samarskii, The Equations of Mathematical Physics [in Russian], Nauka, Moscow (1966).

⁶H. S. Carslaw and J. C. Jaeger, Conduction of Heat in Solids, 2nd Edn., Oxford Univ. Press (1959).

⁷A. P. Prudnikov, Yu. A. Brychkov, and O. I. Marichev, Integrals and Series [in Russian], Nauka, Moscow (1981).

⁸F. W. J. Olver, Asymptotics and Special Functions, Academic Press (1974).

⁹Gu Lun Kun, Dokl. Akad. Nauk SSSR **138**, 263 (1961).

¹⁰G. M. Kudinov, D. E. Temkin, and B. Ya. Lyubov, Fiz. Met. Metalloved. **46**, 540 (1978).

Translated by S. G. Kirsch

Solubility and growth of crystals of rhodochrosite in hydrothermal chloride solutions

V. M. Egorov

Institute of Crystallography, Academy of Sciences of the USSR

(Submitted February 8, 1983; resubmitted November 17, 1983)

Kristallografiya **30**, 161-165 (January-February 1985)

The authors have studied the solubility of MnCO_3 crystals in aqueous 5-8 M solutions of LiCl at 250-400°C and in $\text{LiCl} + \text{NH}_4\text{Cl}$ with a total concentration of 7 M at 300°C. They have investigated the IR spectra of a condensate, formed as a result of dissolving MnCO_3 in aqueous LiCl solution, and constituting a precrystallization phase. They have analyzed the relationship between the degree of association of the particles in the solution and the shape of the equilibrium curves. They have developed a hydrothermal method of growing single crystals of MnCO_3 in aqueous solutions of LiCl and NH_4Cl .

Manganese carbonate, found in nature as the mineral rhodochrosite, is a structural analog of calcite. Single crystals of MnCO_3 are of interest as antiferromagnetics, since the Mn in them occurs only in the form of Mn^{2+} (Ref. 1).

Ikornikova^{2,3} has shown that it is possible to obtain MnCO_3 crystals measuring 5-7 mm by spontaneous crystallization from aqueous solutions of lithium chloride at temperatures up to 450°C and pressures up to 1300 atm. To grow large MnCO_3 crystals on a seed, we need data on the solubility of MnCO_3 in hydrothermal solutions of chlo-

rides, among which, to judge by preliminary experiments, the strongest solvents are solutions of LiCl and NH_4Cl .

This present article is devoted to an investigation of the solubility and growth of MnCO_3 crystals at temperatures from 250 to 400°C and pressures from 700 to 900 kg/cm² in aqueous solutions of LiCl and $\text{LiCl} + \text{NH}_4\text{Cl}$.

SOLUBILITY OF MnCO_3 CRYSTALS

The solubility of rhodochrosite crystals was studied by the weight loss method.

The solvents were salt solutions with molar concentra-